Electron-Transport Properties and Use in Organic Light-Emitting Diodes of a Bis(dioxaborine)fluorene Derivative†

Benoit Domercq,‡,|| Cara Grasso,§ Jose-Luis Maldonado,‡ Marcus Halik,§ Stephen Barlow,§,⊥ Seth R. Marder*,‡,§,⊥ and Bernard Kippelen*,‡,||

Optical Sciences Center and Department of Chemistry, University of Arizona, Tucson, Arizona 85721

Received: September 17, 2003; In Final Form: December 4, 2003

Bis(dioxaborine)fluorenes (DOB) have been studied as potential electron-transport materials. These materials are reversibly reduced at ca. −1.31 V vs ferrocenium/ferrocene, indicating that they have considerably higher electron affinities than tris(8-hydroxyquinoline)aluminum (AlQ_3). They are also highly fluorescent in both solution and the solid state. Time-of-flight measurements show the room-temperature electron mobility of one example to be 2 orders of magnitude higher than the commonly used electron-transport material AlQ_3. Organic light emitting diode (OLED) devices based on the dioxaborine and poly(9-vinylcarbazole) have been fabricated and show a red emission that can be attributed to an exciplex or a charge-transfer complex formed between the two organic components. Förster energy transfer from the exciplex or the charge-transfer complex to a phthalocyanine dopant in the dioxaborine electron-transport layer leads to a near-infrared-emitting OLED.

Introduction

Tris(8-hydroxyquinoline)aluminum, AlQ_3, is one of the most widely employed molecular electron-transport (ET) materials in organic light-emitting diodes (OLEDs). However, it has a rather low electron mobility of ca. 10^{-6} $cm^2/(V\cdot s)$,[1] and its relatively low electron affinity (EA) means that molecular oxygen can act as a trap and impair the electron-transport properties.[2] ET materials with EAs higher than that of oxygen are desirable since the charge carriers—the radical anions of the ET molecules—will then be stable with respect to electron-transfer reactions with molecular oxygen. The quest for new electron-transport materials for organic electronics applications has focused recently on small-molecule[3−5] or liquid-crystal derivatives of oxadiazoles.[6] Although electron mobilities as high as 10^{-3} $cm^2/(V\cdot s)$ have been observed in liquid-crystalline oxadiazoles,[6] these materials still have rather low electron affinities (around 2.2 eV) which render the electron injection difficult and allow for the molecular oxygen to act as a trap for electron transport. Furthermore, they are not compatible with some of the available low-work-function metals such as magnesium because of poor adhesion properties.

2,2-Difluoro-1,3,2(2*H*)-dioxaborines are heterocycles that can be regarded as β-diketonate complexes of boron difluoride. As shown in Scheme 1, the formal negative charge on the boron leaves a formal positive charge in the β-diketonate part of the molecule; accordingly dioxaborines have been shown to act as good acceptors, both in an electron-transfer sense,[7,8] and as π-acceptors when conjugated through their 4-position.[9,10] We have recently been investigating a series of compounds in which two dioxaborine units are bridged by various conjugated π-systems and have previously reported the mixed-valence anion

SCHEME 1: Synthesis of Bis(dioxaborine)fluorenes, 3

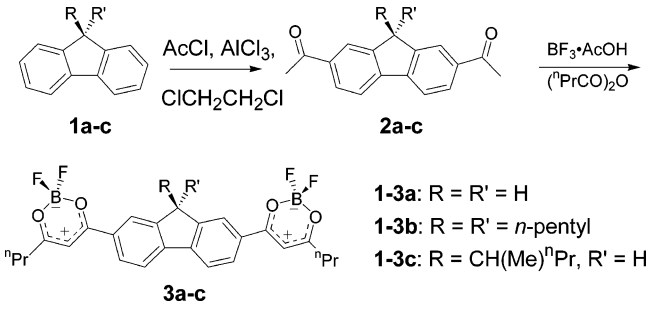

formed by one such species[11] and the two-photon-absorbing properties of others.[12−14] Here we report on our investigations of the ET properties of a bis(dioxaborine)fluorene (DOB). We first present the electronic, thermal, charge-transport, and electrical properties of the material. We then report results obtained using this compound as an ET material in OLEDs in which red emission is observed from an exciplex or charge-transfer complex between the ET material and poly(9-vinylcarbazole). Finally, we show how a near-infrared (NIR) dopant can be used to fabricate a NIR-emitting OLED using energy transfer from this exciplex/charge-transfer complex.

Results and Discussion

Synthesis and Molecular Characterization. Three bis(dioxaborines) with fluorene-2,7-diyl bridges, **3a**−**c** (Scheme 1), were synthesized from the appropriate 2,7-diacetylfluorene derivatives, **2a**−**c**, using a previously described method for dioxaborine synthesis.[15] The diacetyl species, **2a**−**c**, were obtained under standard Friedel−Crafts conditions, with the precursor alkylated fluorenes **1b** and **1c** obtained from fluorene by treatment with the appropriate alkyl bromide in the presence of potassium hydroxide in dimethyl sulfoxide. This paper concentrates on the electronic properties of **3c** and its use in organic light-emitting diodes; the branched alkyl substitution on the 9-position of the fluorene bridge was designed to reduce

† Part of the special issue "Alvin L. Kwiram Festschrift".

‡ Optical Sciences Center.

§ Department of Chemistry.

|| Current address: School of Electrical and Computer Engineering, Georgia Institute of Technology, Atlanta, GA 30332-0250.

⊥ Current address: School of Chemistry and Biochemistry, Georgia Institute of Technology, Atlanta, GA 30332-0400.

10.1021/jp036779r CCC: $27.50
Published on Web 03/09/2004

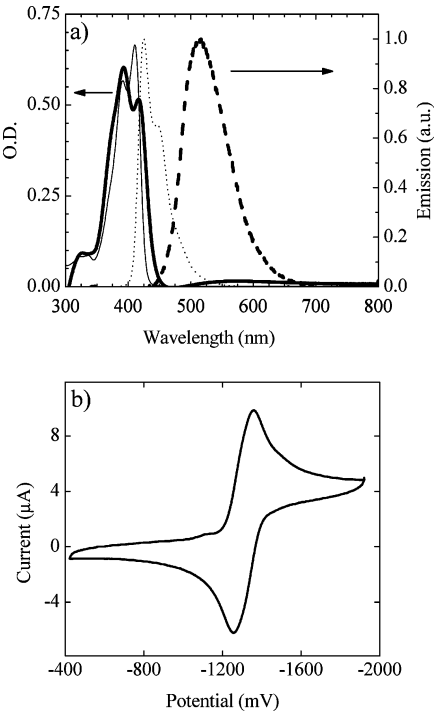

Figure 1. (a) Absorption (solid lines) and photoluminescence (dashed lines) of a 70 nm thick film of **3c** (thick lines) and a solution of **3c** in dichloromethane (thin lines) at a concentration of 7.8×10^{-6} M. (b) Cyclic voltammogram of **3c** in a 0.1 M MeCN solution of $[^nBu_4N]^+[PF_6]^-$ recorded at a scan rate of 50 mV s^{-1}. The potentials shown are relative to ferrocenium/ferrocene.

the tendency of the material to crystallize, and to impart high solubility in organic solvents.

DSC measurements (10 °C/min) show amorphous samples of **3c** undergo a glass transition at 73 °C, followed by recrystallization (variable, but at 119 °C or above), and finally melt at 211 °C. Multiple heating/cooling cycles show that the material is stable in this temperature range. TGA measurements (10 °C/min) show weight loss onset at ca. 283 °C.

Solutions of **3a**−**c** show structured absorptions with the main peak at ca. 410 nm, with emission peaks at ca. 420 nm (Figure 1a, thin lines). All three compounds **3a**−**c** are highly fluorescent (blue) with fluorescence quantum yields in dichloromethane solution of ca. 70%; a value of 72% was determined for **3c**. The absorption of a thin amorphous film of **3c** (70 nm thick), obtained by deposition onto a glass substrate in a vacuum chamber under a vacuum of 10^{-6} Torr, shows a structured absorption peaking at 417 nm with a vibrational subband resolvable at 392 nm (Figure 1a, thick lines). Excitation of this film with a broad-band UV lamp gives a green photoluminescence characterized by a structureless peak with a maximum at 510 nm (Figure 1a). Presumably the differences between the solution and solid-state spectra reflect some intermolecular interactions in the solid films.[16]

Cyclic voltammetry in acetonitrile (Figure 1b) reveals that **3a**−**c** all show a reversible redox feature characterized by a half-wave potential of $E_{1/2} = -1.31$ V vs ferrocenium/ferrocene. We attribute this feature to overlapping **3**/$[\mathbf{3}]^-$ and $[\mathbf{3}]^-/[\mathbf{3}]^{2-}$ redox couples and were unable to resolve any separation between the two processes using cyclic voltammetry, differential pulse voltammetry, or Oysteryoung square-wave voltammetry. The $E_{1/2}$ values indicate that bis(dioxaborines) are considerably more readily reduced than AlQ_3 (ca. −2.30 V in 1:1 acetonitrile/benzene[17]) and, moreover, the potential is comparable to what we observe for the reduction of molecular oxygen in organic solvents.

The HOMO and LUMO levels for **3c** were estimated from the electrochemical, absorption, and photoluminescence data in solution as 6.8 and 3.8 eV, respectively, with respect to vacuum.[18] The energy level of the LUMO respect to vacuum is, therefore, compatible with higher work function metal such as aluminum (4.0 eV) or silver (4.2 eV).

Electron-Transport Properties. The electron mobility of a composite material, **3c**:PBMA (4:1) [PBMA = poly(butyl methacrylate)] was measured using the time-of-flight (TOF) technique, using indium tin oxide (ITO) as electrodes and a 337 nm laser source. The transient time was measured at several different applied fields using a 20 μm thick sample. Because the transient photocurrents were dispersive, the transit times were determined from the double logarithmic plot of the transient photocurrent,[19] being defined as the time at which the slopes of the photocurrent at short and long times undergo a significant change (see inset of Figure 2a). The electron drift mobility μ was calculated from the transit time t_t according to the equation $\mu = d^2/t_tV$, where d is the sample thickness and V is the applied voltage.

As shown in Figure 2b, the electron mobility was found to decrease with increasing electric field. This type of behavior is contrary to that seen in many organic photoconductors where μ typically increases with field; however, similar behavior has been observed in several organic materials including oxadiazole-based liquid crystals[6] and polymers,[20] and certain organometallic polymers.[21] Within the framework of the Borsenberger−Bässler disorder formalism, where it is assumed that energies and positions of transport molecules follow Gaussian distributions,[22−24] the implication of the observed field dependence is that the width of the Gaussian characterizing positional disorder is unusually large due to large variation in intersite distances and/or that the Gaussian describing energetic disorder is unusually narrow.[25] Large positional disorder results in a negative field dependence of the mobility at low field since higher field favors forward hopping and inhibits faster routes for carriers involving shorter hops transverse to the electric field. The electron mobility values measured are 2 orders of magnitude higher than those of the well-known small molecule ET material, AlQ_3. For instance, the electron mobility of AlQ_3 at 40 V/μm has been reported to be between 1.6×10^{-6} and 5.0×10^{-6} $cm^2/(V\cdot s)$,[1,2] where **3c** has a mobility of 1.8×10^{-4} $cm^2/(V\cdot s)$.

The electrical properties of **3c** have been studied in a ET-only single layer device using ITO (indium tin oxide) and Mg:Ag as electrodes. A 100 nm thick film of **3c** was thermally evaporated onto ITO-coated glass substrates, and a 250 nm thick film of a Mg:Ag alloy (10:1) was then evaporated through a mask to define devices with 0.1 cm^2 active area. Test devices were also made in which the **3c** layer was replaced by AlQ_3 (100 nm). The current densities measured in the devices with **3c** are systematically higher than those of AlQ_3 devices (Figure 3a): for instance, the current densities measured at 70 V/μm for **3c** and AlQ_3 devices are 40 and 7 mA/cm^2, respectively. Moreover, electrical stability studies of the **3c**-based device show that, after an initial burn-in, the electrical characteristics are stable (Figure 3b). It is worth noting that these experiments have been done in air.

Organic Light-Emitting Diodes. The high fluorescent quantum efficiency of **3c**, combined with its good ET properties, suggests DOBs as candidates for incorporation into OLEDs. When **3c** is used as the ET layer (ETL) in a device with structure ITO/TPD/ETL/Mg:Ag [TPD = 4,4′-bis(phenyl-*m*-tolylamino)-

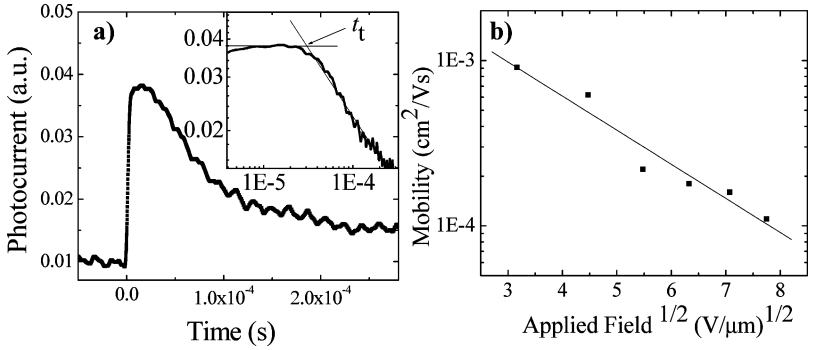

Figure 2. Time-of-flight electron mobility data for a 20 μm thick sample of **3c**:PBMA (4:1) at room temperature. Transient photocurrent measured at an applied field of 60 V/μm (inset log−log plot of the photocurrent with the transit time marked with an arrow) (left); field dependence of electron mobility (right).

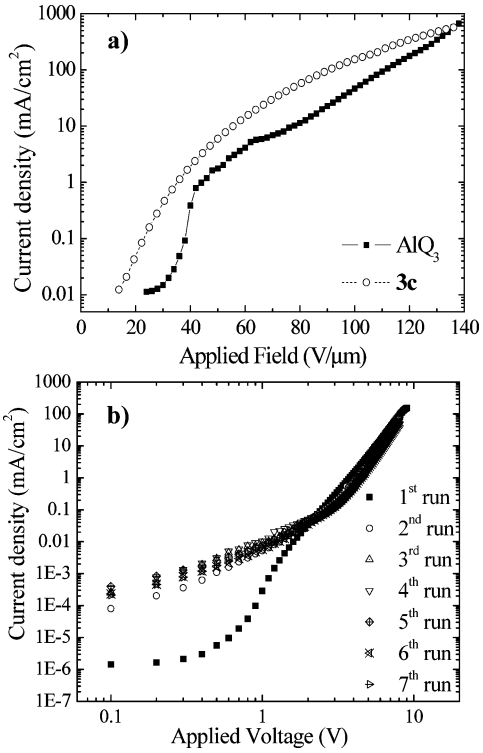

Figure 3. (a) Current density as a function of applied field for an ET-only single layer ITO/(**3c** or AlQ_3)/Mg:Ag (100 nm/250 nm (10:1)) device. (b) Electrical characteristics measured in an ITO/**3c**/Mg:Ag (100 nm/250 nm (10:1)) device for seven consecutive runs.

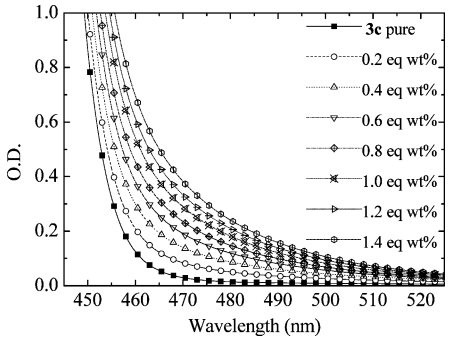

Figure 4. Absorption spectra of a concentrated solution of **3c** in chloroform, showing the effect of adding PVK (10 mg; 0.2 equiv wt %). Growth of a low-energy tail with increasing concentration of PVK is attributed to a PVK:**3c** CT complex. (−■−) pure **3c** (50 mg in 5 cm^3 of $CHCl_3$).

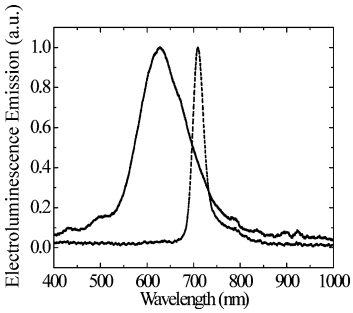

Figure 5. Electroluminescence spectrum of a device with structure ITO/PVK/**3c**/Mg:Ag (50 nm/20 nm/250 nm (10:1)) (solid line) and in a device with structure ITO/PVK/**3c**:AlPc (1 wt %)/Mg:Ag (50 nm/20 nm (1 wt %)/250 nm (10:1)) (dashed line).

biphenyl], we did not observe any measurable light output in the wavelength range 340−1020 nm. The current density shows a diode behavior with a strong rectification, but the measured currents are much lower than in equivalent AlQ_3 devices. Presumably the barriers for hole injection into **3c** and electron injection into TPD are too high to allow formation of either excited TPD or excited **3c** molecules. When a hole-transport-layer (HTL) material with a higher ionization potential such as poly(9-vinylcarbazole) (PVK) (5.9 eV) is employed, red-emitting OLED devices are obtained; the emission of such devices is centered at 627 nm (Figure 5), which corresponds roughly to the energy difference between the HOMO of PVK and the LUMO of **3c** (2.0 eV). The turn-on voltages for the current and for the light output are 1.5 and 9.6 V, respectively. The emission is, therefore, likely to be due to the emission of a charge-transfer (CT) complex formed between the hole-transport (HT) material and **3c**, or to an exciplex formed between these two species. Indeed, it has been shown previously that dioxaborine compounds tend to form charge-transfer complexes with triphenylamine or PVK,[26−28] and detailed comparison of the UV−vis spectra of thin films (Figure 4) does suggest that a CT complex is formed in the present case. This result suggests that, by using HT materials with various ionization potentials, it should be possible to tune the red emission of the OLED device.

Recently, Armstrong and co-workers used phthalocyanines and naphthalocyanines to fabricate NIR OLEDs utilizing Förster energy transfer.[29] We fabricated a similar device using **3c** as the ET material, and using the well-known aluminum phthalocyanine chloride (AlPc) as a NIR-emitting dopant. This dopant was chosen because its absorption spectrum overlaps well with the emission of our red OLED device. AlPc was coevaporated with **3c** at a 1 wt % level. The resulting electroluminescence spectrum of an ITO/PVK/**3c**:AlPc(1 wt %)/Mg:Ag device is shown in Figure 5. Energy transfer from the PVK−**3c** exciplex/CT complex to the NIR dopant AlPc results in the disappearance

of the red emission seen for devices without AlPc; in parallel, the external quantum efficiency increases by a factor of 3 compared to the undoped device. The emission observed is characteristic of AlPc. This increase in quantum efficiency is attributed to the AlPc dopant having a higher fluorescent quantum yield than the CT complex/exciplex.

Summary

We have shown that bis(dioxaborine)fluorenes are promising ET materials for organic electronic applications. We have characterized room-temperature electron mobility in these compounds, and have demonstrated that they can be used as ET material in OLEDs. Red emission in a PVK/DOB device was attributed to a CT complex formed between PVK and DOB, or an exciplex formed between these molecules. We have exploited Förster energy transfer from this CT complex to AlPc to fabricate a NIR-emitting OLED device.

Experimental Section

General. Fluorescence quantum yields were determined in nondeoxygenated dichloromethane solutions using a Spex Fluorlog 3 fluorometer; the measurements were conducted using 9,10-diphenylanthracene in nondeoxygenated cyclohexane as a reference standard ($\eta = 0.70$).[30] Electrochemical measurements were carried out under argon on dry deoxygenated acetonitrile solutions ca. 5×10^{-4} M in analyte and 0.1 M in $[^nBu_4N]^+[PF_6]^-$ using a BAS Potentiostat, a glassy carbon working electrode, a platinum auxiliary electrode, and a silver wire anodized with AgCl as a pseudo reference electrode. Potentials were referenced to ferrocenium/ferrocene by using ferrocene as an internal reference. Details for compounds **2a**−**3a** and **1b**−**3b** have appeared in the supplementary information for refs 12 and 13, respectively.

1,2-Diacetyl-9-(1-methyl-*n*-butyl)fluorene (2c). 2-Bromopentane (19.93 g, 0.132 mol), KOH (16.83 g, 0.300 mol), and water (10 mL) were added to a solution of fluorene (20.00 g, 0.120 mol) in dimethyl sulfoxide (200 mL), and the mixture was stirred for 20 h. Water was added and the solution was extracted with ether (3×100 mL). The organic layer was washed with water (3×150 mL), dried with $MgSO_4$, and evaporated under reduced pressure to yield a yellow liquid containing 9-(1-methyl-*n*-butyl)fluorene (**1c**, 82% pure according to GC−MS; total crude yield 26.3 g). The crude product was used in the next step without further purification. Acetyl chloride (16.95 g, 0.216 mol) was added over 30 min to a suspension of $AlCl_3$ (32.89 g) and 1,2-dichloroethane (200 mL) cooled to 5 °C. Crude **1c** (24.30 g, 0.1028 mol) was then added slowly. The reaction mixture was stirred for 1 h at room temperature and for 2 h at 40 °C, and was then poured carefully onto ice (500 cm^3). The organic layer was washed with water, 0.02 M NaOH, and again with water (200 mL), and evaporated under reduced pressure. Water and hexane (200 mL each) were added to the flask; the resulting white solid was collected and was recrystallized from ethanol (18.54 g, 0.058 mol, 52% overall from fluorene). ^{1}H NMR (500 MHz, $CDCl_3$) δ 8.10 (s, 2H), 7.97 (dd, $J = 7.8$ and 1.5 Hz, 2H), (dd, $J = 7.8$ and 3.9 Hz, 2H), 4.01 (d, $J = 2.4$ Hz, 1H), 2.64 (s, 3H), 2.63 (s, 3H), 2.45 (m, 1H), 1.46−1.29 (m, 4H), 0.89 (t, $J = 6.8$ Hz, 3H), and 0.58 (d, $J = 6.8$ Hz, 3H). ^{13}C NMR ($CDCl_3$, 125 MHz) δ 197.8, 148.4, 147.2, 145.1, 144.7, 136.5, 136.3, 128.1, 128.0, 124.8, 124.2, 120.5, 120.4, 52.6, 36.8, 36.6, 26.8, 20.9, 15.7, and 14.1. Anal. Calcd for $C_{22}H_{24}O_2$: C, 82.46; H, 7.55. Found: C, 82.70; H, 7.63.

4,4′-[9-(1-Methyl-*n*-butyl)fluorene-2,7-diyl]di(6-*n*-propyl-2,2-difluoro-1,3,2(2*H*)-dioxaborine) (3c). $BF_3(CH_3COOH)_2$ (7.03 g, 37.4 mmol) was added to butyric anhydride (18.38 g, 112 mmol), and the mixture was heated to 60 °C. Over a period of 4 h, **2c** (3.00 g, 9.36 mmol) was added to the flask in small portions. The reaction was stirred for a further 14 h at 60 °C, after which time the mixture was allowed to cool. The resulting solids were collected via filtration, recrystallized from acetic acid, and purified by column chromatography on silica gel using 3:1 dichloromethane/hexanes. ^{1}H NMR (500 MHz, $CDCl_3$) δ 8.23 (s, 1H), 8.21 (s, 1H), 8.09 (t, $J = 6.5$ Hz, 2 H), 7.89 (q, $J = 4.1$ Hz 2H), 6.65 (s, 1H), 6.63 (s 1H), 4.07 (s 1H), 2.64 (t, $J = 7.6$ Hz 4H), 2.47 (m, 1H) 1.84 (m, 4H), 1.35 (m, 4H), 1.05 (t, $J = 7.3$ Hz 6H), 0.91 (t, $J = 6.9$ Hz, 3H), 0.61 (d, $J = 6.9$ Hz, 3H). ^{13}C NMR ($CDCl_3$, 125 MHz) δ 195.7, 182.3, 182.2, 149.2, 148.1, 146.8, 146.5, 131.3, 131.2, 128.7, 128.6, 125.5, 125.1, 121.5, 121.4, 97.1, 53.0, 40.0, 36.9, 36.5, 20.9, 19.7, 19.6, 15.8, 14.2, and 13.7. Anal. Calcd for $C_{30}H_{35}B_2O_4F_4$: C, 64.78; H, 6.16. Found: C, 64.62, H, 5.98. HRMS Calcd for $C_{30}H_{35}B_2O_4F_4$: 556.2590. Found: 556.2592.

Mobility Measurements. Samples were prepared by dissolving **3c** and poly(butyl methacrylate) (PBMA) (4:1 wt ratio) in dichloromethane. PBMA was used to ensure the mechanical properties necessary for processing **3c** into thick films. The solution was filtered through a syringe with a 0.2-μm pore size filter and evaporated under reduced pressure. The blend was then dried under vacuum for 16 h. Samples were prepared by melting a small amount of material between two ITO-coated glass slides at a temperature of 140 °C. Calibrated glass spacers of 20 μm were used to ensure a uniform sample thickness. Finally, samples were sealed with quick-setting epoxy adhesive. Further details of the time-of-flight experiment have been reported elsewhere.[31]

OLED Fabrication and Characterization. Compound **3c** was purified by chromatography and recrystallized prior to use. PVK (Aldrich, average M_w 1 100 000) was purified twice by precipitation from its chloroform solution by methanol. Aluminum phthalocyanine chloride (Aldrich) was purified by zone sublimation prior to use. The indium tin oxide (ITO) coated glass with a sheet resistance of 20 Ω/□ (Colorado Concept Coatings LLC) was cut into 2.54×2.54 cm^2 substrates and then ultrasonically cleaned in a bath of acetone and ethanol sequentially for 1 h. A 250 nm thick SiO_2 stripe was deposited on a portion of the substrate to allow device testing without short-circuiting. The substrates were then cleaned again using the above-described process and then air plasma treated to remove any residual organic contaminant and to enhance the ITO work function. The substrates were then loaded onto a 4 in. diameter substrate holder. The holder was loaded into a vacuum chamber with a pressure of 10^{-6} Torr during deposition. The deposition rate and the thickness were measured with a quartz control monitor located near the substrate holder.

Acknowledgment. This work is based upon work supported in part by the STC program of the National Science Foundation under Agreement No. DMR-0120967. We also gratefully acknowledge ONR, the NSF for a CAREER grant to B.K., NASA through University Alabama Hunstville, and DUREL Corp. for their financial support.

References and Notes

(1) Kepler, R. G.; Beeson, P. M.; Jacobs, S. J.; Anderson, R. A.; Sinclair, M. B.; Valencia, V. S.; Cahill, P. A. *Appl. Phys. Lett.* **1995**, *66*, 3618.

(2) Malliaras, G. G.; Shen, Y.; Dunlap, D. H.; Murata, H.; Kafafi, Z. H. *Appl. Phys. Lett.* **2001**, *79*, 2582.

(3) Cea, P.; Hua, Y.; Pearson, C.; Wang, C.; Bryce, M. R.; Royo, F. M.; Petty, M. C. *Thin Solid Films* **2002**, 275.

(4) Tokuhisa, H.; Era, M.; Tsutsui, T. *Adv. Mater.* **1998**, *10*, 404−407.

(5) Adachi, C.; Tsutsui, T.; Saito, S. *Appl. Phys. Lett.* **1989**, *55*, 1489−1491.

(6) Zhang, Y.-D.; Jespersen, K. G.; Kempe, M.; Kornfield, J. A.; Barlow, S.; Kippelen, B.; Marder, S. R. *Langmuir* **2003**, *19*, 6534−6536.

(7) Rapta, P.; Erentová, K.; Stasko, A.; Hartmann, H. *Electrochim. Acta* **1994**, *39*, 2251−2259.

(8) Chow, Y. L.; Johansson, C. I.; Zhang, Y.-H.; Gautron, R.; Yang, L.; Rassat, A.; Yang, S.-Z. *J. Phys. Org. Chem.* **1996**, *9*, 7−16.

(9) Kammler, R.; Bourhill, G.; Jin, Y.; Bräuchle, C.; Görlitz, G.; Hartmann, H. *J. Chem. Soc., Faraday Trans.* **1996**, *92*, 945−947.

(10) Halik, M.; Hartmann, H. *Chem. Eur. J.* **1999**, *5*, 2511−2517.

(11) Risko, C.; Barlow, S.; Coropceanu, V.; Halik, M.; Brédas, J.-L.; Marder, S. R. *Chem. Commun.* **2003**, 194−195.

(12) Halik, M.; Wenseleers, W.; Grasso, C.; Stellacci, F.; Zojer, E.; Barlow, S.; Brédas, J.-L.; Perry, J. W.; Marder, S. R. *Chem. Commun.* **2003**, 1490−1491.

(13) Zojer, E.; Wenseleers, W.; Halik, M.; Grasso, C.; Barlow, S.; Perry, J. W.; Marder, S. R.; Brédas, J.-L. *Chem. Phys. Chem.*, in press.

(14) Zojer, E.; Wenseleers, W.; Pacher, P.; Barlow, S.; M. Halik; Grasso, C.; Perry, J. W.; Marder, S. R.; Brédas, J.-L. *J. Phys. Chem. B,* in press.

(15) Görlitz, G.; Hartmann, H. *Heteroatom Chem.* **1997**, *8*, 147−155.

(16) Since fluorenones have been found to be readily formed as green-emitting impurities in polyfluorenes (for example, see: Scherf, U.; List, E. J. W. *Adv. Mater.* **2002**, *14*, 477 and Romaner, L.; Pogantsch, A.; Scandiucci de Freitas, P.; Scherf, U.; Gaal, M.; Zojer, E.; List, E. J. W. *Adv. Funct. Mater*. **2003**, *13*, 597), it is necessary to exclude the possibility that the green emission of solid **3c** is due to similar impurities. However, we observed similar green emission from a range of other bis(dioxaborines) (which like **3c** are blue-emitting in solution) in the solid state, including biphenyl and dihydrophenanthrene-bridged species in which fluorenone formation is not possible, strongly suggesting that the differences between the solid-state and solution emission spectra of **3c** are not due to fluorenone impurities.

(17) Anderson, J. D.; McDonald, E. M.; Lee, P. A.; Anderson, M. L.; Ritchie, E. L.; Hall, H. K.; Hopkins, T.; Nash, E. A.; Wang, J.; Padias, A.; Thayumanavan, S.; Barlow, S.; Marder, S. R.; Jabbour, G.; Shaheen, S.; Kippelen, B.; Peyghambarian, N.; Wightman, R. M.; Armstrong, N. R. *J. Am. Chem. Soc.* **1998**, *120*, 9646.

(18) The LUMO energy of **3c** was estimated assuming $E_{1/2}(\mathrm{TPD}^+/\mathrm{TPD}) - E_{1/2}(\mathbf{3c}/\mathbf{3c}^-) = E_{\mathrm{HOMO}}(\mathrm{TPD}) - E_{\mathrm{LUMO}}(\mathbf{3c})$, using a value of +0.26 V vs ferrocenium/ferrocene for the value of $E_{1/2}(\mathrm{TPD}^+/\mathrm{TPD})$ (Hreha, R. D.; Haldi, A.; Domercq, B.; Malagoli, M.; Barlow, S.; Brédas, J.-L.; Kippelen, B.; Marder, S. R. *Adv. Funct. Mater*. **2003**, *13*, 967) and a value of 5.4 eV (from UV-PES) for E_{HOMO}(TPD) (see ref 17). The HOMO energy of **3** was estimated by adding the average of the solution absorption and fluorescence maxima to the LUMO energy.

(19) Scher, H.; Montroll, E. W. *Phys. Rev. B* **1975**, *12*, 2455.

(20) Hou, S. J.; Gong, X.; Chan, W. K. *Macromol. Chem. Phys.* **1999**, *200*, 100−105.

(21) Kokil, A.; Shiyanovskaya, I.; Singer, K. D.; Weder, C. *J. Am. Chem. Soc.* **2002**, *124*, 9978.

(22) Bässler, H. *Phys. Status Solidi B* **1993**, *B175*, 15−56.

(23) Borsenberger, P. M.; Magin, E. H.; van der Auweraer, M.; de Schryver, F. C. *Phys. Status Solidi A* **1993**, *A140*, 9.

(24) Bässler, H. *Mol. Cryst. Liq. Cryst.* **1994**, *252*, 11.

(25) Pautmeier, L.; Richtert, R.; Bässler, H. *Synth. Met.* **1990**, *37*, 271.

(26) Halm, J. M.; DeLorme, J. H. *Photogr. Sci. Eng.* **1979**, *23*, 252.

(27) Goliber, T. E.; Perlstein, J. H. *J. Chem. Phys.* **1984**, *80*, 4162−4167.

(28) Goliber, T. E.; Perlstein, J. H. *Photogr. Sci. Eng.* **1982**, *26*, 236.

(29) Flora, W. H.; Hall, H. K.; Armstrong, N. R. *J. Chem. Phys. B* **2002**, *107*, 1142.

(30) Meech, S. R.; Phillips, D. *J. Photochem.* **1983**, *23*, 193−217.

(31) Maldonado, J.-L.; Bishop, M.; Fuentes-Hernandez, C.; Caron, P.; Domercq, B.; Zhang, Y.-D.; Barlow, S.; Thayumanavan, S.; Malagoli, M.; Brédas, J.-L.; Marder, S. R.; Kippelen, B. *Chem. Mater.* **2003**, *15*, 994−999.